JACS
JOURNAL OF THE AMERICAN CHEMICAL SOCIETY
Article
pubs.acs.org/JACS

Urea-Functionalized M_4L_6 Cage Receptors: Anion-Templated Self-Assembly and Selective Guest Exchange in Aqueous Solutions

Radu Custelcean,*[,†] Peter V. Bonnesen,[†,‡] Nathan C. Duncan,[†] Xiaohua Zhang,[†] Lori A. Watson,[§] Gary Van Berkel,[†] Whitney B. Parson,[†] and Benjamin P. Hay[†]

[†]Chemical Sciences Division, Oak Ridge National Laboratory, Oak Ridge, Tennessee 37831-6119, United States
[‡]Center for Nanophase Materials Sciences, Oak Ridge National Laboratory, Oak Ridge, Tennessee 37831-6494, United States
[§]Department of Chemistry, Earlham College, Richmond, Indiana 47374-4095, United States

Supporting Information

ABSTRACT: We present an extensive study of a novel class of *de novo* designed tetrahedral M_4L_6 (M = Ni, Zn) cage receptors, wherein internal decoration of the cage cavities with urea anion-binding groups, via functionalization of the organic components L, led to selective encapsulation of tetrahedral oxoanions EO_4^{n-} (E = S, Se, Cr, Mo, W, n = 2; E = P, n = 3) from aqueous solutions, based on shape, size, and charge recognition. External functionalization with *t*Bu groups led to enhanced solubility of the cages in aqueous methanol solutions, thereby allowing for their thorough characterization by multinuclear (^{1}H, ^{13}C, ^{77}Se) and diffusion NMR spectroscopies. Additional experimental characterization by electrospray ionization mass spectrometry, UV−vis spectroscopy, and single-crystal X-ray diffraction, as well as theoretical calculations, led to a detailed understanding of the cage structures, self-assembly, and anion encapsulation. We found that the cage self-assembly is templated by EO_4^{n-} oxoanions ($n \geq 2$), and upon removal of the templating anion the tetrahedral M_4L_6 cages rearrange into different coordination assemblies. The exchange selectivity among EO_4^{n-} oxoanions has been investigated with ^{77}Se NMR spectroscopy using $^{77}SeO_4^{2-}$ as an anionic probe, which found the following selectivity trend: $PO_4^{3-} \gg CrO_4^{2-} > SO_4^{2-} > SeO_4^{2-} > MoO_4^{2-} > WO_4^{2-}$. In addition to the complementarity and flexibility of the cage receptor, a combination of factors have been found to contribute to the observed anion selectivity, including the anions' charge, size, hydration, basicity, and hydrogen-bond acceptor abilities.

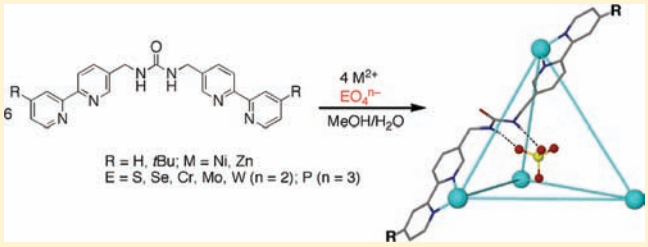

INTRODUCTION

Research in the area of self-assembled cages has undergone remarkable progress in the past two decades.[1] These molecular containers, also called capsules or flasks, present a number of attractive features: (i) they can be easily assembled in one step by combining relatively simple components via reversible supramolecular interactions; (ii) they contain confined chemical environments that can serve as platforms for host−guest chemistry, molecular recognition, sensing, or catalysis; and (iii) they are often aesthetically appealing. While research on self-assembled cages was initially focused mainly on their synthesis and characterization, more recently the attention has shifted to the exploration of their chemical and biological applications.[1] Toward this goal, parallels are often drawn between molecular containers and protein receptors or enzymes. Indeed, some synthetic cage molecules have been demonstrated to mimic their natural counterparts in their abilities to bind substrates, stabilize reactive species, or accelerate chemical transformations.[2] However, the synthetic molecular containers reported to date rarely combine the two critical elements characteristic to natural receptors and enzymes: internal cavities precisely functionalized with hydrogen-bonding groups, and highly efficient and selective guest binding in aqueous environments.[3]

Among the various supramolecular interactions that can be employed for cage self-assembly, metal−ligand coordination bonds are relatively strong and directional, thereby offering a higher degree of control and predictability.[1a] The M_4L_6 tetrahedron, self-assembled from four metal centers and six ditopic ligands serving as vertices and edges, respectively, represents the prototypical coordination cage. Following the discovery of the first M_4L_6 cage in 1988,[4] many other examples of such tetrahedral assemblies have been demonstrated.[5−8] These tetrahedral cages can bear negative or positive charge, thereby serving as potential hosts for cationic or anionic guests, respectively. In either case, charge-diffuse monoions are preferentially encapsulated, as multicharged anions are associated with large dehydration energies that cannot be fully compensated by binding inside the typically hydrophobic cavities of M_4L_6 cages.[7b,9]

Recent work in our group has focused on the study of anion recognition and separation with self-assembled receptors.[10]

Received: January 20, 2012
Published: April 30, 2012

   dx.doi.org/10.1021/ja300677w | J. Am. Chem. Soc. 2012, 134, 8525−8534

Scheme 1. M_4L_6 Cages Investigated in This Study

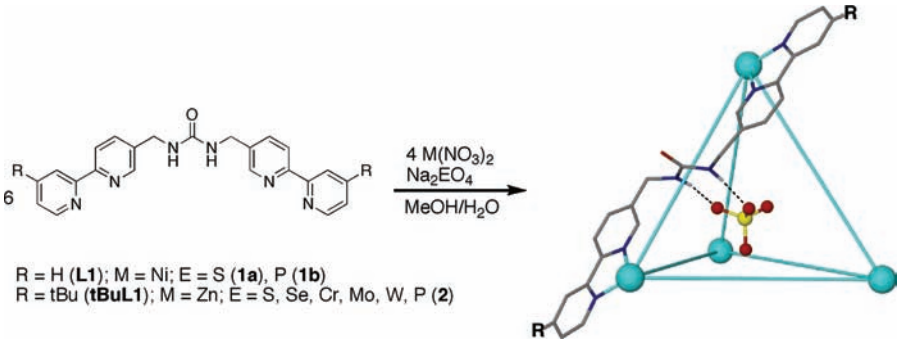

Along this line, we have been particularly interested in the development of novel metal-based anion receptors[11,12] that can function selectively and efficiently in aqueous environments.[13] This is a challenging task, as many anions have large free energies of hydration, and thus are difficult to bind and extract from water.[14] Toward this end, cage receptors that can fully encapsulate the anions, thereby shielding them from the competitive aqueous environment, are especially promising.[15,16] M_4L_6 cages in particular appeared to us ideal for binding tetrahedral anions based on the shape match between the cage host and the anion guest. Indeed, a number of positively charged M_4L_6 cages have been demonstrated to bind tetrahedral anions, such as BF_4^-, ClO_4^-, or $FeCl_4^-$.[6,7,8c] All these anions, however, have relatively low charge density, and their binding was generally observed in nonaqueous solvents. Furthermore, their encapsulation inside the cages' hydrophobic cavities is primarily based on optimal filling of the cavity volume, rather than on specific interactions. We reasoned that selective and efficient binding of the more hydrophilic, multicharged tetrahedral oxoanions[17] (e.g., SO_4^{2-}, SeO_4^{2-}, CrO_4^{2-}, PO_4^{3-}) from water requires a new generation of M_4L_6 cage receptors strategically functionalized with complementary binding groups. Besides advancing the basic understanding of self-assembled cages, effective implementation of this approach may also lead to anion separation applications, as many tetrahedral oxoanions are relevant to environment and energy.[17]

Guided by *de novo* computer-aided design, we recently developed the sulfate-encapsulating tetrahedral cage $[Ni_4(L1)_6(SO_4)]^{6+}$ (**1a**, Scheme 1).[18] Functionalization of the L1 edges with ureas resulted in an internal cavity decorated with 12 NH hydrogen-bond donors complementary to the tetrahedral sulfate anion. This led to exceptionally strong sulfate binding in water, on a par with sulfate-binding protein. However, a number of fundamental questions remained unanswered: (1) Does the cage display, as designed, shape selectivity for tetrahedral oxoanions? (2) Does the encapsulated anion act as a template to cage self-assembly? (3) What fundamental factors govern anion selectivity is this class of cage receptors? These questions will be addressed in the present paper based on an extensive study of the prototype cage **1a** and the next-generation cages $[Zn_4(tBuL1)_6(EO_4)]^{(8-n)+}$ (E = S, Se, Cr, Mo, W, n = 2; E = P, n = 3) (**2**). Experimental investigation by multinuclear (^{1}H, ^{13}C, ^{77}Se) and diffusion NMR spectroscopies, electrospray ionization mass spectrometry (ESI-MS), UV–vis spectroscopy, and single-crystal X-ray diffraction (XRD), as well as theoretical analysis by density functional theory (DFT) calculations and molecular dynamics (MD) simulations, led in the end to a detailed understanding of the structures, self-assembly, and anion encapsulation chemistry of this novel class of cage receptors. We found that, in direct contrast to previously reported ion-binding M_4L_6 cages favoring relatively hydrophobic, neutral or monocharged guests, the cage receptors described here preferentially encapsulate strongly hydrophilic, multicharged anions, due to hydrogen-bond stabilization inside the urea-functionalized cavities.

EXPERIMENTAL SECTION

Materials and Methods. All chemicals were at least reagent grade and were used as received from the suppliers without further purification unless otherwise noted. Solutions were prepared using volumetric glassware, and calibrated Eppendorf pipets were used to deliver specific volumes of reagent solutions. All ^{1}H (499.717 MHz), ^{13}C, and ^{31}P NMR experiments were performed on a Varian VNMRS 500 NMR spectrometer at 23 °C using a 5-mm AutoX DB probe, with spinner turned off, unless otherwise noted. Spectra recorded in $CDCl_3$ were referenced to internal tetramethylsilane (0 ppm) for proton spectra, and to 77.23 ppm for carbon spectra. Spectra obtained in CD_3OD–D_2O mixtures were referenced to 3.31 and 49.15 ppm unless otherwise noted. Low-resolution ESI-MS was performed on 5 μM cage solutions in 1:1 water–methanol (v/v) using a Sciex API 165 instrument operated at 5 kV, with a sample injection rate of 20 μL/min. High-resolution electrospray ionization ion mobility time-of-flight mass spectrometry (ESI-IM-TOFMS) was performed on 2.5 μM solutions in 1:1 water–methanol (v/v) using a SYNAPT HDMS (Waters Corp., Manchester, UK) equipped with a NanoMate 100 system (Advion BioSciences, Inc. Ithaca, NY). The sample flow rate was 500 nL/min. A voltage of 1.4 kV and a gas pressure of 0.3 psi were employed. Spectra were acquired in positive polarity mode, externally calibrated, and processed using the MassLynx software version 4.1 (Waters Corp.). UV–vis spectra were collected with a Cary 50 UV–vis spectrophotometer.

^{77}Se NMR Experiments. $Na^{77}SeO_4$ and $Zn^{77}SeO_4$ (99.2 atom % ^{77}Se) were prepared as described in the Supporting Information. All ^{77}Se experiments (except diffusion experiments described below) were acquired at a frequency of 95.4 MHz at 23.0 °C on the Varian VNMRS 500. All ^{77}Se chemical shifts were referenced externally to neat Me_2Se (0.0 ppm) contained in a sealed tube. For the $[Zn_4(tBuL1)_6(^{77}SeO_4)](^{77}SeO_4)_3$ cage complex in 2:1 v/v CD_3OD–D_2O, the selenate anion inside the cage is generally observed as a singlet at 1044.2 ppm, whereas the three selenates outside the cage are generally observed as a somewhat broader singlet at 1046.5 ppm. The pw90 was measured to be 13.0 μs at a transmitter power level of 56 for selenate both inside and outside the cage. Inversion–recovery (T_1) experiments on the $[Zn_4(tBuL1)_6(^{77}SeO_4)](^{77}SeO_4)_3$ cage complex in 2:1 v/v CD_3OD–D_2O showed the T_1 for $^{77}SeO_4$ outside and inside the cage to be 6.78 ± 0.66 and 15.38 ± 1.66 s, respectively. Accordingly, for ^{77}Se acquisition parameters, a recycle delay of 120 s and a 10.83 μs (75°) pulse at a transmitter power level of 56 were used in all exchange experiments. Using these parameters, typically a 3.4(1):1 ratio for selenate outside to selenate inside the cage was observed, following the

dx.doi.org/10.1021/ja300677w | J. Am. Chem. Soc. 2012, 134, 8525–8534

collection of at least 500 transients, and the average of at least five separate integrations.

Diffusion NMR Spectroscopy. Diffusion NMR measurements were carried out at 298 K on a Bruker Avance 400 spectrometer using a gradient amplifier with a maximum gradient of 54.1 G/cm. Reference ^{1}H and ^{77}Se (76.31 MHz) NMR spectra of the samples were taken prior to diffusion experiments. The pulse length used for observation of the selenium signal was 14.0 μs for a 90° pulse with a recycle delay of 45s. The Stebpgp1s (STimulated Echo BiPolar Gradient Pulse) program from Bruker Biospin was used for the DOSY NMR using gradients varied linearly from 5% up to 95% in 16 steps, with 64 scans per step for ^{1}H, and 300 scans per step for ^{77}Se. For the ^{1}H measurements, the diffusion time (Δ) was set at 200 ms, and the gradient length (δ) was set at 3.6 ms. For the ^{77}Se measurements, Δ and δ values were in the range of 0.4−2.5 s and 3.6−9.6 ms, respectively. The diffusion coefficients were determined using the Simfit algorithm from Bruker Biospin.

NMR Analysis of Cage Self-Assembly. All stock solutions of *t*BuL1 at 30−33 mM in CD_3OD, $Zn(NO_3)_2{\cdot}4H_2O$ at 41−44 mM in D_2O, and the sodium salt of the anion of interest at 27−65 mM in D_2O were prepared and used within a 2-week time frame. The experiments were designed such that 0.500 mL of *t*BuL1 in CD_3OD is first delivered to the NMR tube, followed by addition of the $Zn(NO_3)_2{\cdot}4H_2O$ in D_2O solution (0.240 to 0.250 mL, the exact volume depending on the concentration of the stock solution), such that the CD_3OD-D_2O is close to a v/v ratio of 2:1. The sodium salts were at a concentration in D_2O such that 40−105 μL quantities would deliver 1 equiv of anion. An example of a typical NMR experiment designed to probe the cage self-assembly is as follows: to 16.1 μmol (6 equiv) of *t*BuL1 in 0.500 mL of CD_3OD in a 5-mm tube was added 10.7 μmol (4 equiv) of $Zn(NO_3)_2{\cdot}4H_2O$ in 0.241 mL of D_2O, and the proton spectrum was recorded to verify the formation of the intermediate coordination complex between zinc nitrate and *t*BuL1. After a minimum of 5 min, 1 equiv (2.69 μmol) of Na_2SeO_4 contained in 48.3 μL of D_2O was added, and after mixing for 20 s, the proton spectrum was recorded within 3−4 min. Cages of the form $[Zn_4(t\text{BuL1})_6(EO_4)](EO_4)_3$ (E = S, Se) were also directly prepared by adding the stoichiometric amount of $ZnEO_4$ dissolved in D_2O to 0.500-mL solutions of *t*BuL1 in CD_3OD. For the more basic phosphate anion, the added D_2O solutions of $Zn(NO_3)_2{\cdot}4H_2O$ and Na_2HPO_4 were buffered at pH 9.5 with borax (0.100 M $Na_2B_4O_7$ 99.5%).

^{77}Se NMR Analysis of Anion Exchange Using ^{77}Se-Enriched Selenate. For each exchange experiment, a solution of the $[Zn_4(t\text{BuL1})_6(^{77}SeO_4)](^{77}SeO_4)_3$ cage complex was first prepared by adding 118.0 μL of 88.9 mM stock solution of $Zn^{77}SeO_4$ in D_2O to 0.500 mL of a 31.45 mM solution of *t*BuL1 in CD_3OD in 5-mm NMR tubes. After mixing and allowing to age for at least 30 min, the proton spectrum was recorded to ensure that the cage complex had been cleanly generated. Next, a specific volume of 0.100 M $Na_2B_4O_7$ in D_2O was added (between 92 and 113 μL, the precise volume depending on the concentration of the exchanging anion solution), and the resulting solution was thoroughly mixed. The proton spectrum was then recorded, followed by an overnight ^{77}Se acquisition (minimum of 500 transients, using the acquisition parameters described above) to determine the baseline ratio of selenate outside to selenate inside the cage (average of at least five integrations.) To perform the anion exchange, a precise volume between 19 and 40 μL of freshly ($\lesssim$3 h) prepared solutions of anhydrous Na_2SO_4, $Na_2CrO_4{\cdot}4H_2O$, $Na_2MoO_4{\cdot}2H_2O$, $Na_2WO_4{\cdot}2H_2O$, or $Na_2HPO_4{\cdot}2H_2O$ in 0.100 M $Na_2B_4O_7$ in D_2O was added to the tube, and the resulting solution was thoroughly mixed. In the cases of chromate and hydrogen phosphate, 1 equiv of anion was added; for the other anions, 2 equiv of anion was added. The CD_3OD/D_2O volume ratio of the final solutions was nominally 2:1 in all experiments. Proton spectra were recorded at least twice over a period of 20 min to observe any changes, and then the ^{77}Se acquisition was recorded overnight, with a minimum of 600 transients being collected. The peaks for the selenate outside and selenate inside the cage were then integrated, and the ratio (as the average of at least five integrations) was compared to the baseline ratio.

RESULTS AND DISCUSSION

Anion-Templated Self-Assembly of $[Ni_4(L1)_6(EO_4)](NO_3)_{8-n}$ Cages (E = S, P; *n* = 2, 3). A solution containing L1, $Ni(NO_3)_2$, and Na_2SO_4 in a 6:4:1 molar ratio in H_2O/MeOH led upon slow evaporation to crystallization of $[Ni_4(L1)_6(SO_4)](NO_3)_6$ (**1a**$(NO_3)_6$). Single-crystal XRD analysis revealed the formation of a cage with quasitetrahedral symmetry (C_3 true symmetry), with slightly different Ni−Ni distances of 11.69 and 11.70 Å, and Ni−Ni−Ni angles of 59.96, 60.00, and 60.02°. This minor distortion from the ideal tetrahedral symmetry is likely a consequence of packing forces in the crystal. However, the observed perturbation in this case is significantly smaller compared to the previously reported cage **1a**$(SO_4)_3$.[18] While the crystal packing in the previous structure was dominated by relatively strong interactions between the external sulfate anions and the cages, the extra-cage nitrate anions in the present structure are highly disordered, resulting in a more loosely packed crystal. Once again, as predicted by molecular design, the encapsulated sulfate accepts 12 hydrogen bonds from the six urea groups functionalizing the cage cavity, with each urea binding an edge of the sulfate.[19] The observed N−H···O hydrogen bond distances and angles are very similar with the corresponding values in **1a**$(SO_4)_3$, ranging between 2.04 and 2.08 Å, and 165.2 and 174.2°, respectively.

Having established the sulfate encapsulation by the $Ni_4(L1)_6$ cage, we next turned our attention to investigating the ability of the cage to encapsulate other tetrahedral oxoanions. The phosphate anion, with size and hydrogen-bonding preferences similar to sulfate, was selected as the next target. Slow evaporation of a H_2O/MeOH solution containing L1, $Ni(NO_3)_2$, and NaH_2PO_4 in a 6:4:1 molar ratio resulted in crystallization of $[Ni_4(L1)_6(PO_4)](NO_3)_5$ (**1b**$(NO_3)_5$), as determined by single-crystal XRD (Figure 1). This structure

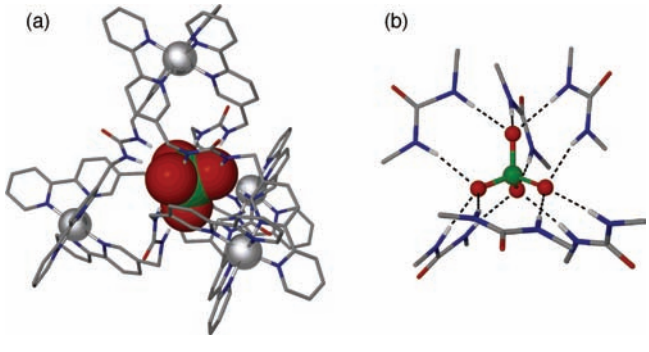

Figure 1. Crystal structure of **1b**$(NO_3)_5$. (a) Tetrahedral $Ni_4(L1)_6$ cage encapsulating a PO_4^{3-} anion. (b) Phosphate binding by 6 urea groups forming 12 NH···O hydrogen bonds.

is essentially isomorphous with **1a**$(NO_3)_6$, containing a quasitetrahedral $Ni_4(L1)_6$ cage with observed Ni−Ni distances of 11.63 and 11.69 Å, and Ni−Ni−Ni angles of 59.83, 60.00, and 60.34°. The encapsulated phosphate is fully deprotonated, despite the fact that under the acidic conditions used for crystallization (pH $\approx$ 4), the phosphate anion exists preponderantly in its diprotonated form. This suggests that the hydrogen-bonding microenvironment inside the cage has a strongly stabilizing effect on PO_4^{3-}, essentially shifting its basicity by a few orders of magnitude.[20] As with the sulfate cage

dx.doi.org/10.1021/ja300677w | J. Am. Chem. Soc. 2012, 134, 8525−8534

analogue, and in agreement with the molecular design, the phosphate orientation is inverted with respect to the tetrahedral cage, with the P−O bonds pointing to the centers of the four triangular faces rather than to the Ni(bpy)$_3$ vertices. The phosphate accepts 12 urea NH hydrogen bonds with relatively linear geometry (N−H···O angles range between 165.8 and 174.2°), and N−H···O contact distances of 1.95−2.06 Å, which are slightly shorter than those observed for the sulfate analogue. This structure thus represents a rare example of a fully deprotonated phosphate coordinatively saturated by 12 hydrogen bonds.[21]

While the tetrahedral cages form in the presence of the SO_4^{2-} or PO_4^{3-} anions, spectroscopic data indicates that the empty $Ni_4(L1)_6$ cage does not persist upon removal of the anionic guest, but it rearranges into other coordination assemblies with the $[Ni_2(L1)_3]_n^{4n+}$ stoichiometry.[1h,22] The visible absorption spectrum of a solution containing 6 equiv of L1 and 4 equiv of $Ni(NO_3)_2$, but no sulfate, is virtually indistinguishable from that of the sulfate-containing cage **1a**$(NO_3)_6$ in H_2O/MeOH (1:1), with absorption maxima observed at 522 and 795 nm (Supporting Information). These values are very similar to the absorption maxima of 519 and 789 nm reported for Ni(bpy)$_3^{2+}$, thereby confirming that all Ni^{2+} cations in solution are chelated by three bpy groups from L1. However, these data cannot distinguish among the various $[Ni_2(L1)_3]_n^{4n+}$ stoichiometries possible. More informative was ESI-MS analysis of H_2O/MeOH (1:1) mixtures containing L1 and $Ni(NO_3)_2$ in a 3:2 ratio, as required for the formation of the $[Ni_2(L1)_3]_n^{4n+}$ coordination assemblies. Specifically, high-resolution ESI-IM-TOFMS identified a relatively intense peak at m/z = 326.6 corresponding to the $Ni_2(L1)_3^{4+}$ ion, as indicated by the good match between the observed and calculated isotopic distributions (Figure 2).

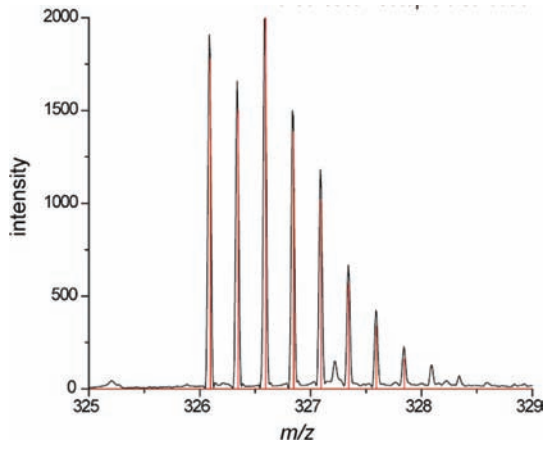

Figure 2. High-resolution ESI-MS: overlay of the calculated (red) and observed (black) peaks for the $Ni_2(L1)_3^{4+}$ ion.

Furthermore, ion mobility analysis, a technique that allows ions with the same m/z to be separated based on their size difference, found no additional ionic species with the mass-to-charge ratio of 326.6 (Supporting Information). Thus, these results provide supporting evidence for the tetrahedral $Ni_4(L1)_6$ cage rearrangement into $Ni_2(L1)_3$ upon removal of the templating anion. A similar guest-controlled interconversion between an M_4L_6 tetrahedral cage and an M_2L_3 helicate had previously been observed by Raymond et al.[23] Unfortunately, despite numerous attempts, we were not able to isolate the $Ni_2(L1)_3$ in crystalline form and prove unequivocally its formation by XRD analysis.

Considering that the latest data suggests the $Ni_4(L1)_6^{8+}$ cage does not persist in solution after the removal of the encapsulated sulfate, a reevaluation of the sulfate binding constant is in order here. Based on competition experiments with Ba^{2+}, the apparent sulfate association constant (K_{app}) had been estimated around $(6 \pm 1) \times 10^6$ M^{-1}.[18] Since it now appears that the $Ni_4(L1)_6^{8+}$ cage rearranges into other coordination assemblies, such as $Ni_2(L1)_3^{4+}$ (Scheme 2), the

Scheme 2. Putative Reaction Equilibria Involving the $[Ni_4(L1)_6(SO_4)]^{6+}$ Cage in Aqueous Solutions[a]

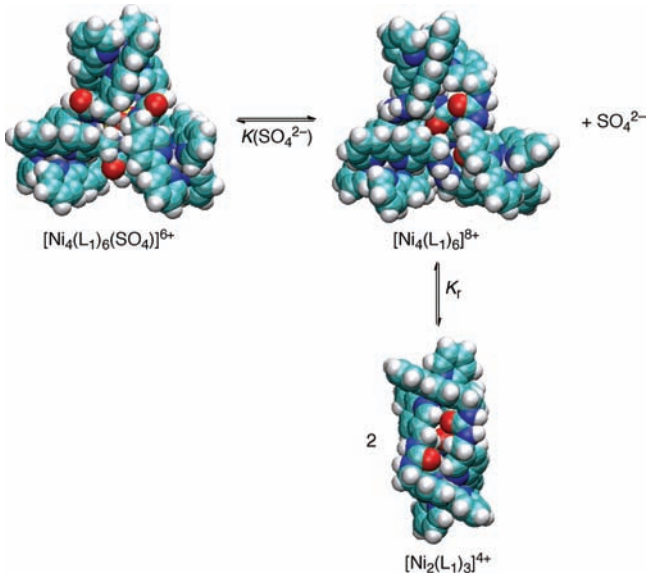

[a]All structures were obtained by taking representative snapshots from the MD simulations (Supporting Information). C, H, N, O, Ni, and S atoms are shown in cyan, white, blue, red, silver, and yellow, respectively.

apparent constant can be defined as $K_{app} = K_r K(SO_4^{2-})$, where K_r is the equilibrium constant for the rearrangement of 2 equiv of $Ni_2(L1)_3^{4+}$ into $Ni_4(L1)_6^{8+}$, and $K(SO_4^{2-})$ is the actual sulfate binding constant by the putative $Ni_4(L1)_6^{8+}$ cage. Unfortunately, the value of K_r remains unknown at this time, which precludes us from obtaining an exact value for $K(SO_4^{2-})$. However, considering that no trace of the $Ni_4(L1)_6^{8+}$ ion could be detected by mass spectrometry, we can assume the concentration of the empty cage in solution is negligible, which implies that $K_r \ll 1$. It thus follows that $K(SO_4^{2-}) \gg (6 \pm 1) \times 10^6$ M^{-1}. This value thus represents a lower limit estimate of the association constant for sulfate binding by $Ni_4(L1)_6^{8+}$.

Anion-Templated Self-Assembly of $[Zn_4(tBuL1)_6(EO_4)](NO_3)_{8-n}$ Cages (E = S, Se, Cr, Mo, W, n = 2; E = P, n = 3). While the prototype L1 ligand and the corresponding $[Ni_4(L1)_6(SO_4)]^{6+}$ cage provided the proof of principle for *de novo* design of self-assembled cage receptors for encapsulation of tetrahedral oxoanions, the limitations of this system quickly became apparent. In particular, the presence of the paramagnetic Ni^{2+} centers rendered the use of NMR spectroscopy impractical, thereby precluding a detailed study of the cage structure and anion selectivity in solution. Our attempts to self-assemble L1 with diamagnetic Zn^{2+} or Fe^{2+}

dx.doi.org/10.1021/ja300677w | J. Am. Chem. Soc. 2012, 134, 8525−8534

metal cations resulted in the formation of intractable precipitates.[24] Due to these limitations, we sought to prepare a derivative of L1 that would self-assemble with the diamagnetic Zn^{2+} into soluble tetrahedral cages amenable to NMR analysis. We hypothesized that a derivative of L1 containing *tert*-butyl groups attached to the bpy moieties would display improved solubility. We therefore proceeded with the synthesis of this second-generation ligand (Supporting Information). The resulting ligand (*t*BuL1) is indeed substantially more soluble than L1 in polar organic solvents such as methanol, enabling us to monitor the cage self-assembly by NMR.

When dissolved in 2:1 v/v CD_3OD-D_2O, the free *t*BuL1 ligand features a broad NMR singlet at δ 4.45 attributable to the methylene protons. Upon addition of six equivalents of zinc nitrate in D_2O to 4 equiv of *t*BuL1 in CD_3OD, the ^1H NMR revealed the formation of a stable but nonsymmetrical complex within a few minutes (Figure 3b). The broad singlet at δ 4.45

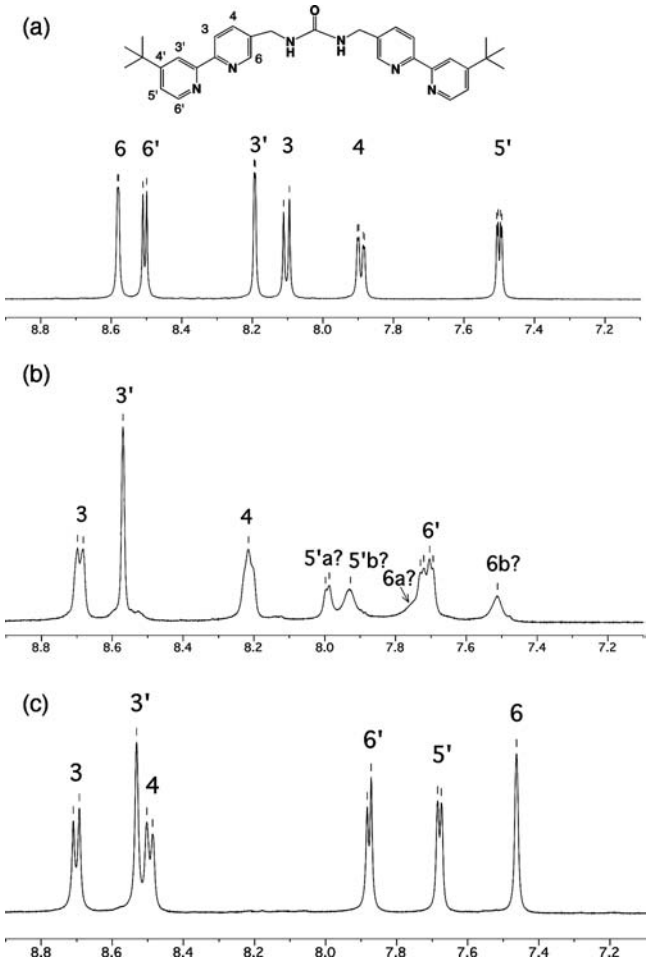

Figure 3. Aromatic regions of the ^1H NMR spectra of (a) free *t*BuL1, (b) $[Zn_2(tBuL1)_3]_n(NO_3)_{4n}$, and (c) $[Zn_4(tBuL1)_6(SO_4)](NO_3)_6$ in 2:1 CD_3OD-D_2O.

corresponding to the $-CH_2-$ of the free ligand *t*BuL1 split into two unsymmetrical broad doublets centered at δ 4.29 and 4.07, as the two methylene protons become diastereotopic. All of the previously sharp aromatic resonances of the free ligand shifted and broadened substantially. Thus, it is apparent that some low-symmetry coordination complex or mixture of complexes is formed between the six *t*BuL1 ligands and the four Zn cations, which will be represented here generically as $[Zn_2(tBuL1)_3]_n(NO_3)_{4n}$.

To probe the formation of the tetrahedral $[Zn_4(tBuL1)_6(X^{n-})](NO_3)_{8-n}$ cages ($\mathbf{2}(NO_3)_6$), we added 1 equiv of various NaX or Na_2X salts in D_2O to NMR tubes containing the $[Zn_2(tBuL1)_3]_n(NO_3)_{4n}$ complex in 2:1 v/v CD_3OD-D_2O. In the cases where X was a dinegatively charged tetrahedral oxoanion (EO_4^{2-}; M = S, Se, Cr, Mo, W), in the time needed to add the salt solution to the NMR tube, shake it, and acquire the proton NMR spectrum (typically 4−5 min after addition), a new set of sharp resonances appeared, indicating the formation of a high-symmetry complex (Figure 3c). The proton and carbon NMR spectra in this series of complexes are very similar, with only very slight differences in the chemical shifts among them (Supporting Information). However, there are noteworthy changes in the chemical shifts when compared to those of the initial $[Zn_2(tBuL1)_3]_n(NO_3)_{4n}$ complex. Particularly in the aromatic region, there are now six sharp resonances corresponding to the six aromatic protons. The $-CH_2-$ group displays a typical AB pattern consisting of two symmetrical doublets centered at δ 4.71 and 3.97, indicative of the diastereotopic relationship of the two methylene protons. These spectra are consistent with the formation of tetrahedral $[Zn_4(tBuL1)_6(EO_4)](NO_3)_6$ cages templated by the EO_4^{2-} anions. The 2− charge of the tetrahedral anions appears to be critical for the cage formation, as no cage was templated by the ClO_4^- or ReO_4^- tetrahedral monoanions, with their NMR spectra remaining virtually unchanged compared to that of the $[Zn_2(tBuL1)_3]_n(NO_3)_{4n}$ complex even after several days. Other monoanions of different shapes, like F^-, Cl^-, Br^-, I^-, NO_3^- (excess), BF_4^-, PF_6^-, $CH_3CO_2^-$, $CH_3SO_3^-$, or $CF_3SO_3^-$, also did not form the cage. Also, no cage formation was observed in the presence of dinegative anions with shapes other than tetrahedral, such as the trigonal planar CO_3^{2-} and the pyramidal SeO_3^{2-} or SO_3^{2-}.[25] Therefore, it is evident that there is a high degree of shape and charge selectivity in the cage formation, with only tetrahedral oxoanions with charges greater than 1− being able to template the cage self-assembly.

The phosphate anion was also found to template the formation of the tetrahedral cage under buffered conditions (borax, pH ≈ 9). Thus, the $[Zn_2(tBuL1)_3]_n(NO_3)_{4n}$ complex was generated as before, but using about two times more concentrated Zn nitrate solution in D_2O. To that solution was added a nearly equal volume of 100 mM $Na_2B_4O_7$ in D_2O. The $[Zn_2(tBuL1)_3]_n(NO_3)_{4n}$ complex appeared to remain unchanged in the resulting alkaline solution containing 15.7 mM of the $Na_2B_4O_7$ buffer, as judged by ^1H NMR. In this case, upon the addition of 1 equiv of Na_2HPO_4 (together with 100 mM $Na_2B_4O_7$ in D_2O), resonances consistent with the $[Zn_4(tBuL1)_6(PO_4)](NO_3)_5$ cage were observed within 5 min (Supporting Information). It was also noted, however, that resonances due to the free *t*BuL1 ligand also appeared within the same time, with an observed ratio of free *t*BuL1 to cage-bound *t*BuL1 of approximately 11(±1):89(±1). In the same time, a small amount of flocculant precipitate formed, which was likely zinc phosphate based on its very low solubility (K_{sp} = 9.0 × 10^{-33}). We thus surmise that the free *t*BuL1 observed by NMR could be due to the loss of Zn by competitive precipitation of zinc phosphate.[26] It appears that the system reached the equilibrium, as there was no apparent increase in the amount of precipitate or free ligand relative to the cage-bound ligand over the course of 2 days.

dx.doi.org/10.1021/ja300677w | *J. Am. Chem. Soc.* 2012, 134, 8525−8534

Table 1. ESI-MS Peaks Observed (Calculated) for the $[Zn_4(tBuL1)_6(EO_4)](NO_3)_n(EO_4)_m$ Cages from 5 μM Solutions in 1:1 (v/v) H_2O/MeOH

	m/*z*				
E	*n* = 0, *m* = 0	*n* = 0, *m* = 1	*n* = 1, *m* = 0	*n* = 2, *m* = 0	*n* = 3, *m* = 0
S	568.2 (568.2)	876.1 (876.0)	694.3 (694.3)	883.3 (883.4)	1198.4 (1198.5)
Se	575.9 (576.1)	899.9 (899.8)	703.7 (703.7)	895.0 (895.1)	1213.5 (1213.8)
Cr	571.6 (571.6)	886.1 (886.3)	698.1 (698.3)	–	–
Mo	578.7 (578.9)	908.2 (908.1)	707.0 (707.1)	–	–
W	–	–	–	–	–
P	681.6 (681.5)	–	867.3 (867.6)	–	–

Complementary evidence for the formation of the $[Zn_4(tBuL1)_6(EO_4)]^{n+}$ tetrahedral cages was provided by ESI-MS. Thus, analysis of solutions containing 6:4:1 molar ratios of *t*BuL1, $Zn(NO_3)_2$, and Na_2EO_4 (or Na_2HPO_4) in 1:1 (v/v) H_2O/MeOH displayed peaks corresponding to various $[Zn_4(tBuL1)_6(EO_4)](NO_3)_n(EO_4)_m^{(8-n-2m)+}$ cations (Table 1). For example, in the case of sulfate, peaks were observed at *m*/*z* values corresponding to $[Zn_4(tBuL1)_6(SO_4)]^{6+}$, $[Zn_4(tBuL1)_6(SO_4)](SO_4)^{4+}$, $[Zn_4(tBuL1)_6(SO_4)](NO_3)^{5+}$, $[Zn_4(tBuL1)_6(SO_4)](NO_3)_2^{4+}$, and $[Zn_4(tBuL1)_6(SO_4)](NO_3)_3^{3+}$ (Supporting Information). The other EO_4^{n-} anions (n = 2, 3) showed similar results, with the exception of WO_4^{2-}, which displayed no peaks corresponding to the cage. We assume that in this case the cage either does not persist at the very low concentration of the solution under study (5 μM), or it decomposes under the electrospray ionization conditions.[27] No cage formation was evident from dinegative anions of shapes different than tetrahedral, such as SO_3^{2-} or CO_3^{2-}.

Single crystals suitable for XRD were obtained for the $[Zn_4(tBuL1)_6(EO_4)](NO_3)_6$ tetrahedral complexes (E = S (**2a**), Cr (**2b**), and Mo (**2c**)), thereby allowing for a detailed structural characterization of the cage geometry and anion encapsulation. The three cages have isomorphous structures, with the monoclinic $P2_1/n$ space group. The structure of **2a** is illustrated in Figure 4, and relevant geometric parameters for **2a**–**c** are listed in Table 2.

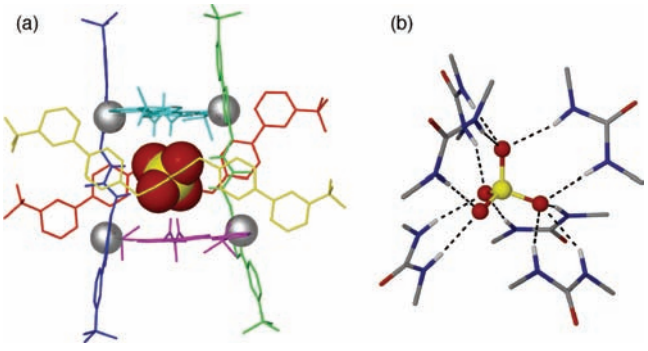

Figure 4. Crystal structure of **2a**. (a) Tetrahedral $Zn_4(tBuL1)_6$ cage encapsulating a SO_4^{2-} anion. (b) Sulfate binding by six urea groups, forming 12 NH···O hydrogen bonds.

The three cages have distorted tetrahedral shapes and almost identical sizes, with the average Zn–Zn edge length varying only slightly among the cages, from 11.92 to 11.95 Å. Each of the three EO_4^{2-} anions is encapsulated in the center of the cage via 12 hydrogen bonds from six urea groups. However, the anion coordination is less symmetrical than in the Ni cage analogues, with five urea groups each binding an O–E–O edge

Table 2. Pertinent Geometric Parameters for the Crystal Structures of 2a–c

	2a (E = S)	**2b** (E = Cr)	**2c** (E = Mo)
d(Zn–Zn) (Å)	11.79–12.34	11.76–12.28	11.74–12.30
	av. 11.95	av. 11.97	av. 11.92
d(NH···O) (Å)	1.97–2.27	1.98–2.28	1.98–2.39
	av. 2.09	av. 2.07	av. 2.10
∠(N–H···O) (deg)	151.1–175.3	145.7–175.0	143.6–174.1
	av. 162.3	av. 161.4	av. 159.2
∠(E–O···H) (deg)	96.1–149.3	92.2–145.0	81.6–145.1
	av. 119.7	av. 115.9	av. 112.5

of the oxoanion, and the sixth urea binding an O vertex (Figure 4b). The hydrogen-bonding parameters are very similar in the three structures, despite the significant difference in the anion sizes. For example, the shortest average NH···O contact distance of 2.07 Å is observed for chromate in **2b**, but the corresponding contact distances for sulfate and molybdate in **2a** and **2c** are only 0.02 and 0.03 Å longer, respectively. Similarly, the average hydrogen-bond donor angles (∠N–H···O) vary only by 3.1° among the three structures. However, there are larger differences among the average hydrogen-bond acceptor angles (E–O···H), which vary from 119.7° for SO_4^{2-} to 112.5° for MoO_4^{2-}. Overall, these X-ray data indicate that the $[Zn_4(tBuL1)_6(EO_4)](NO_3)_6$ tetrahedral cages are structurally quite flexible, distorting their frames to accommodate the different sized EO_4^{2-} anions and optimize their hydrogen bonding by the urea groups.

Diffusion NMR spectroscopy was carried out to obtain further information about the identity of the various coordination assemblies formed in solution. The translational self-diffusion coefficient (D) for the $[Zn_4(tBuL1)_6(SO_4)](NO_3)_6$ cage (**2a**) in 2:1 v/v CD_3OD–D_2O, measured by the stimulated echo diffusion ^1H NMR, was $1.01(7) \times 10^{-10}$ m^2/s. For comparison, at $1.89(16) \times 10^{-10}$ m^2/s, the corresponding D value measured for *t*BuL1 was almost twice as large. Furthermore, for **2a**, a 2D DOSY (diffusion ordered spectroscopy) plot showed that all the cage peaks have the same diffusion coefficient (Supporting Information), indicating the presence of a single supramolecular aggregate in solution. Based on these data, a hydrodynamic radius (r) of 13.6 ± 1.4 Å was estimated for **2a** using the Stokes–Einstein equation (eq 1), where k is the Boltzmann constant, T the temperature, and η the solvent viscosity.[28] This experimental value for r is in good agreement with the 14.2(2) Å calculated value for the tetrahedral cage $[Zn_4(tBuL1)_6(SO_4)]$, obtained from MD simulations.[29]

$$D = k_B T/6\pi\eta r \quad (1)$$

dx.doi.org/10.1021/ja300677w | J. Am. Chem. Soc. 2012, 134, 8525–8534

Diffusion NMR spectroscopy is often used as a powerful tool for probing encapsulation phenomena in molecular cages, by demonstrating that the encapsulated guest has a similar diffusion coefficient as the cage host.[30] This could be achieved in our case by employing $^{77}SeO_4^{2-}$ as an NMR-active anionic probe. ^{77}Se is a spin $^1/_2$ nucleus with generally narrow linewidths over a wide chemical shift range. However, its receptivity at natural abundance of 7.6% is moderately low (about 3.1 times greater than for ^{13}C), and its spin−lattice relaxation times tend to be long. Initial ^{77}Se NMR testing was performed on the $[Zn_4(t\text{BuL1})_6(SeO_4)](SeO_4)_3$ cage using natural abundance zinc selenate in 2:1 v/v CD_3OD-D_2O. Under these conditions it was possible to detect separate peaks for selenate outside (ca. 1046 ppm) and inside (ca. 1044 ppm) the cage in a roughly 3:1 ratio, although the signal-to-noise ratio was quite low. We therefore prepared $Zn^{77}SeO_4$ from elemental Se that was enriched to 99.2 atom % in ^{77}Se (Supporting Information), and subsequently converted it into the $[Zn_4(t\text{BuL1})_6(^{77}SeO_4)](^{77}SeO_4)_3$ cage (**2-Se**).

^1H DOSY of **2-Se** in 2:1 v/v CD_3OD-D_2O yielded a diffusion coefficient D of $0.98(8) \times 10^{-10}$ m^2/s for this cage, which, as expected, is close to the value found for the analogous sulfate-encapsulating cage **2a**. ^{77}Se DOSY[31] of **2-Se** in the same solvent mixture yielded a very similar diffusion coefficient of $0.94(5) \times 10^{-10}$ m^2/s for one of the two distinct $^{77}SeO_4^{2-}$ anions observed, thereby providing strong evidence for its encapsulation inside the cage. On the other hand, a significantly larger diffusion coefficient of $1.8(2) \times 10^{-10}$ m^2/s was measured for the $^{77}SeO_4^{2-}$ anions outside the cage. For comparison, the diffusion coefficient of "free" selenate, measured from a solution of $Zn^{77}SeO_4$ in the same solvent mixture, is 2.7×10^{-10} m^2/s, indicating some degree of ion pairing between the 6+ cage cation and the outside selenate anions.

Anion Exchange by the $[Zn_4(t\text{BuL1})_6(EO_4)]^{(8-n)+}$ Cages (E = S, Se, Cr, Mo, W, n = 2; E = P, n = 3). Although the $[Zn_4(t\text{BuL1})_6(EO_4)]^{(8-n)+}$ cages do not persist in the absence of the encapsulated anions, thereby preventing the measurement of the absolute values for the anion binding constants, competitive exchange of the EO_4^{n-} anions offers an alternative way for measuring the relative anion encapsulation selectivity. In the previous section we had shown that ^{77}Se NMR is a viable method for probing anion encapsulation with this class of self-assembled cages. In this section, we demonstrate that the same technique may be effectively employed for quantitative measurement of anion exchange selectivity.

The exchange experiments were performed by first preparing solutions of the $[Zn_4(t\text{BuL1})_6(^{77}SeO_4)](^{77}SeO_4)_3$ cage complex that were buffered by addition of small volumes (92−113 μL) of 0.100 M $Na_2B_4O_7$ in D_2O, to bring the pH of the solution to around 9.[32] Next, a ^{77}Se NMR spectrum was collected to obtain the $[^{77}SeO_4]_{out}/[^{77}SeO_4]_{in}$ baseline before adding 1 or 2 equiv of Na_2SO_4, Na_2CrO_4, Na_2MoO_4, or Na_2WO_4 in 0.100 M $Na_2B_4O_7$ in D_2O. After addition of the exchanging anion solution, the proton NMR spectrum was recorded, followed by an overnight ^{77}Se acquisition to determine the equilibrium $[^{77}SeO_4]_{out}/[^{77}SeO_4]_{in}$ (Figure 5). The anion exchange reactions under consideration are shown in eq 2.

$$[Zn_4(t\text{BuL1})_6(^{77}SeO_4)]^{6+} + EO_4^{2-} \overset{K_{ex}}{\rightleftharpoons} [Zn_4(t\text{BuL1})_6(EO_4^{2-})]^{6+} + {}^{77}SeO_4^{2-} \quad (2)$$

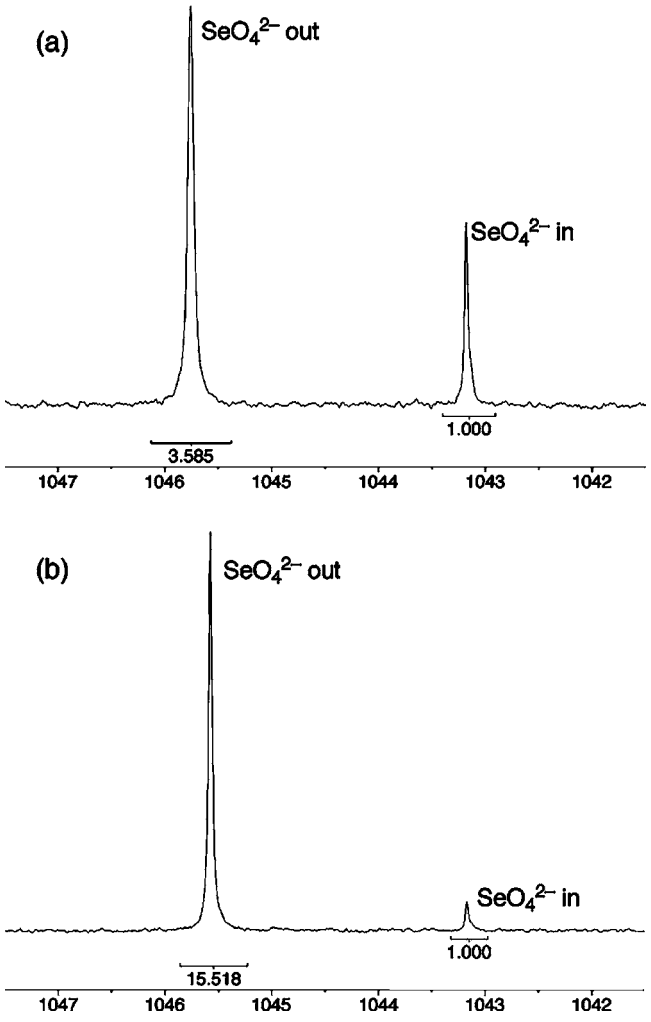

Figure 5. Exchange of $^{77}SeO_4^{2-}$ by CrO_4^{2-} in the $[Zn_4(t\text{BuL1})_6(^{77}SeO_4)](^{77}SeO_4)_3$ cage, monitored by ^{77}Se NMR: (a) before and (b) after the addition of 1 equiv of CrO_4^{2-}.

Based on the initial and the equilibrium $[^{77}SeO_4]_{out}/[^{77}SeO_4]_{in}$ ratios measured by NMR, K_{ex} was then calculated according to eq 3 (see Supporting Information for details of the calculations):

$$K_{ex} = \frac{[Zn_4(t\text{BuL1})_6(EO_4^{2-})]^{6+}_{eq}[^{77}SeO_4^{2-}]_{eq}}{[Zn_4(t\text{BuL1})_6(^{77}SeO_4)]^{6+}_{eq}[EO_4^{2-}]_{eq}} \quad (3)$$

The initial and equilibrium $[^{77}SeO_4]_{out}/[^{77}SeO_4]_{in}$ ratios measured by NMR, and the K_{ex} values corresponding to selenate exchange by the EO_4^{2-} anions (E = S, Cr, Mo, W) are shown in Table 3. According to these data, the relative cage affinity for the EO_4^{2-} anions is $CrO_4^{2-} > SO_4^{2-} > SeO_4^{2-} > MoO_4^{2-} > WO_4^{2-}$. Using a similar approach, we also measured the PO_4^{3-}/SeO_4^{2-} anion exchange with the cage, and obtained an apparent K_{ex} = 15.82. This exchange equilibrium constant is denoted as apparent, as under these conditions there are other coexisting protonation equilibria involving phosphate. Though the exact value of K_{ex} for phosphate cannot be determined from the available data, we can estimate that $\log K_{ex} > 4.5$ (Supporting Information). Thus, the binding of PO_4^{3-} is much stronger compared to the EO_4^{2-} anions, as expected based on the enhanced electrostatic attraction of the 8+ cage

dx.doi.org/10.1021/ja300677w | J. Am. Chem. Soc. 2012, 134, 8525−8534

Table 3. $^{77}SeO_4^{2-}$ Exchange by EO_4^{2-} (E = S, Cr, Mo, W) in the $[Zn_4(tBuL1)_6(^{77}SeO_4)](^{77}SeO_4)_3$ Cage, Measured by ^{77}Se NMR

anion	no. equiv added per equiv cage[a]	$[^{77}SeO_4]_{out}/[^{77}SeO_4]_{in}$ initial[b]	final[c]	K_{ex}[d]
SO_4^{2-}	2	3.522	13.65	7.21
CrO_4^{2-}	1	3.569	15.42	40.10
MoO_4^{2-}	2	3.485	4.115	0.27
WO_4^{2-}	2	3.561	3.670	0.04

[a]In all cases, after addition of the anion solution, the total D_2O volume was 0.250 mL and the total CD_3OD volume was 0.500 mL. [b]From the average of at least five integrations for spectra obtained after a minimum of 500 transients; maximum uncertainty in all integrals is ±5%. [c]From the average of at least 5 integrations for spectrum obtained after a minimum of 600 transients; all solutions were clear with no precipitates; maximum uncertainty in all integrals is ±5%. [d]K_{ex} calculated with eq 3; uncertainty is ±14%.

for the higher-charged phosphate, as well as the greater basicity of this anion.

To rationalize the observed selectivity trend among the EO_4^{2-} anions, several factors need to be taken into account. First, regarding the cage host, the important factors are its rigidity and the complementarity of the binding cavity for the various encapsulated anions. Second, concerning the anionic guests, there are some intrinsic properties associated with the anions, such as their size (expressed here as the E−O bond length), their basicity (pK_a of HEO_4^-),[33] and their free energy of hydration[34] (Table 4). Also included in Table 4 are the gas-phase thermodynamic parameters for EO_4^{2-} binding by six urea groups, calculated using DFT at the B3LYP level of theory; these parameters define the intrinsic hydrogen-bond-accepting abilities of the EO_4^{2-} anions toward the urea functional groups. All these intrinsic factors define the baseline selectivity, on top of which operate any existing host−guest recognition phenomena.

As indicated by the X-ray structural analysis of **2a−c**, the tetrahedral cage has a high degree of complementary for tetrahedral oxoanions, manifested by the formation of 12 NH···O hydrogen bonds. There is, however, relatively little difference in binding geometry among the three EO_4^{2-} anions analyzed (Table 3), despite their significantly different sizes. This can be explained by the high flexibility of the cage, which distorts its structure to accommodate the different sized EO_4^{2-} anions and optimize their binding by the urea groups. There are some subtle geometric differences, though, in the observed hydrogen-bonding parameters. Thus, the average NH···O contact distance is slightly shorter for CrO_4^{2-} than for the other anions. On the other hand, both the average hydrogen-bond donor (N−H···O) and acceptor (E−O···H) angles are most favorable for SO_4^{2-}.[35] These geometric differences, however, are too small to fully account for the observed anion exchange selectivity in the $[Zn_4(tBuL1)_6(EO_4)]^{6+}$ cage series, and other factors must play significant roles.

The calculated gas-phase free energy of reactions for the binding of the EO_4^{2-} anions by six urea groups decreases when going from the smallest sulfate to the largest tungstate anion. This is expected based on the corresponding decrease in anions' charge density with the increase in their size. The observed anion exchange selectivity generally follows the same trend, which is consistent with an anti-Hofmeister bias. Anti-Hofmeister selectivity in anion binding from water corresponds to a more stabilizing environment for the anions in the binding cavity of the receptor relative to the external aqueous environment.[14] Such a behavior is expected for the urea-functionalized $[Zn_4(tBuL1)_6(EO_4)]^{6+}$ cages, whose binding cavities offer a highly complementary, strongly stabilizing environment to tetrahedral EO_4^{2-} anions. The only anion in the series that does not follow the anti-Hofmeister selectivity trend is CrO_4^{2-}. In this regard, it should be noted that chromate is by far the strongest base in the series, based on the known pK_a values of HEO_4^-. It is most instructive to compare CrO_4^{2-} with SeO_4^{2-}, which are essentially identical in size, and have similar free energies of hydration. However, CrO_4^{2-} is preferred over SeO_4^{2-} by a factor of 40, which could be attributed to the much stronger basicity of the former. A similar comparison can be made between MoO_4^{2-} and WO_4^{2-}, which have virtually identical size, but the more basic MoO_4^{2-} is preferred over WO_4^{2-} by a factor of 7. On the other hand, between SO_4^{2-} and SeO_4^{2-}, which have similar basicity, the smaller SO_4^{2-} is bound more strongly.

CONCLUSIONS

A novel class of M_4L_6 tetrahedral cages acting as selective anion receptors in competitive aqueous solutions has been thoroughly investigated experimentally by multinuclear NMR spectroscopy, DOSY, ESI-MS, UV−vis, and X-ray crystallography, as well as theoretically by DFT calculations and MD simulations. Internal functionalization of the cages' cavities with six urea anion-binding groups, guided by *de novo* computer-aided design, resulted in selective encapsulation of tetrahedral EO_4^{n-} oxoanions (E = S, Se, Cr, Mo, W, n = 2; E = P, n = 3) against anions of different shapes and charges, including F^-, Cl^-, Br^-, I^-, NO_3^-, BF_4^-, ClO_4^-, ReO_4^-, PF_6^-, $CH_3CO_2^-$, $CH_3SO_3^-$, $CF_3SO_3^-$, CO_3^{2-}, SO_3^{2-}, and SeO_3^{2-}. In a notable contrast to previously reported ion-binding M_4L_6 cages that favored encapsulation of relatively hydrophobic monocharged ions, the cage receptors described here showed preferential

Table 4. Properties of the EO_4^{2-} Anions

EO_4^{2-}	d(E−O),[a] Å	$\Delta G°_{hy}$,[b] kJ/mol	ΔG_{rxn}(urea$_6$),[c] kJ/mol	ΔH_{rxn}(urea$_6$),[c] kJ/mol	$pK_a(HEO_4^-)$,[d]
SO_4^{2-}	1.47(4)	−1080	−530.5	−770.8	1.99
CrO_4^{2-}	1.64(4)	−950	−519.0	−762.3	6.51
SeO_4^{2-}	1.63(4)	−900	−501.9	−745.7	1.70
MoO_4^{2-}	1.75(2)	–	−486.0	−729.0	4.24
WO_4^{2-}	1.75(3)	–	−485.9	−732.2	3.50

[a]Average values obtained from Cambridge Structural Database, Version 5.32 (Nov 2010). [b]Free energies of hydration;[34] no values for MoO_4^{2-} and WO_4^{2-} are available. [c]Calculated thermodynamic parameters for the equilibrium reaction: $EO_4^{2-} + 6(urea) \leftrightarrows EO_4(urea)_6^{2-}$. [d]Values obtained from ref 33.

dx.doi.org/10.1021/ja300677w | J. Am. Chem. Soc. 2012, 134, 8525−8534

encapsulation of strongly hydrophilic, multicharged anions, as a consequence of the presence of stabilizing hydrogen-bond donor groups decorating the internal cavities of the cages. Tetrahedral EO_4^{n-} oxoanions (n = 2, 3) have been found to act as templates for the cage self-assembly. In the absence of such templates, no M_4L_6 cages could be observed, and other coordination assemblies formed in solution.

Despite their lack of preorganization, the M_4L_6 cage receptors studied here display remarkable affinities and selectivities for tetrahedral EO_4^{n-} oxoanions in aqueous environments. Though the exact anion binding constants could not be measured due to the instability of the "empty" cages, we estimated a lower limit of $(6 \pm 1) \times 10^6$ M^{-1} for the association constant corresponding to sulfate binding by the $Ni_4(L1)_6^{8+}$ cage receptor. In the case of $[Zn_4(t\text{BuL1})_6(EO_4)]^{6+}$ cages, the relative anion encapsulation selectivity could be assessed from anion exchange experiments monitored by ^{77}Se NMR spectroscopy, using $^{77}SeO_4^{2-}$ as an NMR-active anionic probe. The following anion selectivity trend was found: $PO_4^{3-} \gg CrO_4^{2-} > SO_4^{2-} > SeO_4^{2-} > MoO_4^{2-} > WO_4^{2-}$. The observed trend mostly parallels the decrease in anions' charge densities, which corresponds to an anti-Hofmeister selectivity. Such a behavior is consistent with the presence of a more stabilizing environment for the anions inside the urea-functionalized cages relative to the external aqueous solution. Another factor contributing to the observed selectivity is the structural flexibility of the cages, which can distort their frames to accommodate different-sized anions and optimize their binding by the urea groups. These results suggest that with improved preorganization and structural rigidity, even stronger anion binding and more prominent selectivities may be achievable with this class of cage receptors, potentially leading to applications related to separation of environmentally relevant anions (e.g., sulfate separation from nuclear waste).[36]

■ ASSOCIATED CONTENT

Supporting Information

Detailed experimental and synthetic procedures; NMR (^1H, ^{13}C, ^{77}Se), DOSY, UV−vis, and ESI-MS spectra; energies and coordinates of DFT-optimized structures; details of the MD simulations; and X-ray crystallographic data including CIF files. This material is available free of charge via the Internet at http://pubs.acs.org.

■ AUTHOR INFORMATION

Corresponding Author

custelceanr@ornl.gov

Notes

The authors declare no competing financial interest.

■ ACKNOWLEDGMENTS

This research was sponsored by the Division of Chemical Sciences, Geosciences, and Biosciences, Office of Basic Energy Sciences, U.S. Department of Energy. The synthesis of ^{77}Se-labeled materials, and NMR experiments involving cage formation and anion exchange were conducted at the Center for Nanophase Materials Sciences, which is sponsored at Oak Ridge National Laboratory by the Scientific User Facilities Division, Office of Basic Energy Sciences, U.S. Department of Energy.

■ REFERENCES

(1) Recent reviews on self-assembled containers: (a) Chakrabarty, R.; Mukherjee, P. S.; Stang, P. J. *Chem. Rev.* **2011**, *111*, 6810. (b) Laughrey, Z.; Gibb, B. C. *Chem. Soc. Rev.* **2011**, *40*, 363. (c) Avram, L.; Cohen, Y.; Rebek, J. *Chem. Commun.* **2011**, *47*, 5368. (d) Breiner, B.; Clegg, J. K.; Nitschke, J. R. *Chem. Sci.* **2011**, *2*, 51. (e) Pluth, M. D.; Bergman, R. G.; Raymond, K. N. *Acc. Chem. Res.* **2009**, *42*, 1650. (f) Michito, Y.; Klosterman, J. K.; Fujita, M. *Angew. Chem., Int. Ed.* **2009**, *48*, 3418. (g) Rebek, J. *Acc. Chem. Res.* **2009**, *42*, 1660. (h) Ward, M. D. *Chem. Commun.* **2009**, 4487.

(2) (a) Hastings, C. J.; Backlund, M. P.; Bergman, R. G.; Raymond, K. N. *Angew. Chem., Int. Ed.* **2011**, *50*, 10570. (b) Hastings, C. J.; Backlund, M. P.; Bergman, R. G.; Raymond, K. N. *J. Am. Chem. Soc.* **2010**, *132*, 6938. (c) Bao, X.; Rieth, S.; Stojanovic, S.; Hadad, C. M.; Badjic, J. D. *Angew. Chem., Int. Ed.* **2010**, *49*, 4816. (d) Crisostomo, F. R. P.; Lledo, A.; Shenoy, S. R.; Iwasawa, T.; Rebek, J. *J. Am. Chem. Soc.* **2009**, *131*, 7402. (e) Iwasawa, T.; Hooley, R. J.; Rebek, J. *Science* **2007**, *317*, 493. (f) Pluth, M. D.; Bergman, R. G.; Raymond, K. N. *Science* **2007**, *316*, 85. (g) Yoshizawa, M.; Tamura, M.; Fujita, M. *Science* **2006**, *312*, 251.

(3) (a) Ferrand, Y.; Crump, M. P.; Davis, A. P. *Science* **2007**, *318*, 619. (b) Rehm, T. H.; Schmuck, C. *Chem. Soc. Rev.* **2010**, *39*, 3597.

(4) (a) Saalfrank, R. W.; Stark, A.; Peters, K.; von Schnering, H. G. *Angew. Chem., Int. Ed.* **1988**, *27*, 851. (b) Saalfrank, R. W.; Maid, H.; Scheurer, A. *Angew. Chem., Int. Ed.* **2008**, *47*, 8794.

(5) (a) Caulder, D. L.; Powers, R. E.; Parac, T. N.; Raymond, K. N. *Angew. Chem., Int. Ed.* **1998**, *37*, 1840. (b) Caulder, D. L.; Raymond, K. N. *Acc. Chem. Res.* **1999**, *32*, 975. (c) Davis, A. V.; Fiedler, D.; Ziegler, M.; Terpin, A.; Raymond, K. N. *J. Am. Chem. Soc.* **2007**, *129*, 15354.

(6) (a) Fleming, J. S.; Mann, K. L. V.; Carraz, C.-A.; Psillakis, E.; Jeffery, J. C.; McCleverty, J. A.; Ward, M. D. *Angew. Chem., Int. Ed.* **1998**, *37*, 1279. (b) Paul, R. L.; Bell, Z. R.; Jeffery, J. C.; McCleverty, J. A.; Ward, M. D. *Proc. Natl. Acad. Sci. U.S.A.* **2002**, *99*, 4883. (c) Paul, R. L.; Argent, S. P.; Jeffery, J. C.; Harding, L. P.; Lynam, J. M.; Ward, M. D. *Dalton Trans.* **2004**, 3453. (d) Tidmarsh, I. S.; Taylor, B. F.; Hardie, M. J.; Russo, L.; Clegg, W.; Ward, M. D. *New J. Chem.* **2009**, *33*, 366. (e) Hall, B. R.; Manck, L. E.; Tidmarsh, I. S.; Stephenson, A.; Taylor, B. F.; Blaikie, E. J.; Vander Griend, D. A.; Ward, M. D. *Dalton Trans.* **2011**, *40*, 12132.

(7) (a) Glasson, C. R. K.; Meehan, G. V.; Clegg, J. K.; Lindoy, L. F.; Turner, P.; Duriska, M. B.; Willis, R. *Chem. Commun.* **2008**, 1190. (b) Glasson, C. R. K.; Clegg, J. K.; McMurtrie, J. C.; Meehan, G. V.; Lindoy, L. F.; Motti, C. A.; Moubaraki, B.; Murray, K. S.; Cashion, J. D. *Chem. Sci.* **2011**, *2*, 540.

(8) (a) Mal, P.; Schultz, D.; Beyeh, K.; Rissanen, K.; Nitschke, J. R. *Angew. Chem., Int. Ed.* **2008**, *47*, 8297. (b) Meng, W.; Clegg, J. K.; Thoburn, J. D.; Nitschke, J. R. *J. Am. Chem. Soc.* **2011**, *133*, 13652. (c) Hristova, Y. R.; Smulders, M. M. J.; Clegg, J. K.; Breiner, B.; Nitschke, J. R. *Chem. Sci.* **2011**, *2*, 638.

(9) Parac, T. N.; Caulder, D. L.; Raymond, K. N. *J. Am. Chem. Soc.* **1998**, *120*, 8003.

(10) Custelcean, R. *Top. Curr. Chem.* **2012**, *322*, 193.

(11) Recent reviews on anion receptors: (a) Wenzel, M.; Hiscock, J. R.; Gale, P. A. *Chem. Soc. Rev.* **2012**, *41*, 480. (b) Gale, P. A. *Chem. Commun.* **2011**, *47*, 82. (c) Gale, P. A. *Chem. Soc. Rev.* **2010**, *39*, 3746.

(12) Recent reviews on metal-based self-assembled anion receptors: (a) Mercer, D. J.; Loeb, S. J. *Chem. Soc. Rev.* **2010**, *39*, 3612. (b) Amendola, V.; Fabbrizzi, L. *Chem. Commun.* **2009**, 513. (c) Steed, J. W. *Chem. Soc. Rev.* **2009**, *38*, 506.

(13) Kubik, S. *Chem. Soc. Rev.* **2010**, *39*, 3648.

(14) (a) Custelcean, R. *Curr. Opin. Solid State Mater. Sci.* **2009**, *13*, 68. (b) Custelcean, R.; Moyer, B. A. *Eur. J. Inorg. Chem.* **2007**, 1321.

(15) Recent reviews on cage receptors for anions: (a) Kang, S. O.; Llinares, J. M.; Day, V. W.; Bowman-James, K. *Chem. Soc. Rev.* **2010**, *39*, 3980−4003. (b) Ballester, P. *Chem. Soc. Rev.* **2010**, *39*, 3810.

(16) (a) Rajbanshi, A.; Moyer, B. A.; Custelcean, R. *Cryst. Growth. Des.* **2011**, *11*, 2702. (b) Custelcean, R.; Bock, A.; Moyer, B. A. *J. Am. Chem. Soc.* **2010**, *132*, 7177. (c) Custelcean, R.; Remy, P. *Cryst. Growth. Des.* **2009**, *9*, 1985.

(17) Katayev, E. A.; Ustynyuk, Y. A.; Sessler, J. L. *Coord. Chem. Rev.* **2006**, *250*, 3004.
(18) Custelcean, R.; Bosano, J.; Bonnesen, P. V.; Kertesz, V.; Hay, B. P. *Angew. Chem., Int. Ed.* **2009**, *48*, 4025.
(19) Custelcean, R.; Moyer, B. A.; Hay, B. P. *Chem. Commun.* **2005**, 5971.
(20) Busschaert, N.; Gale, P. A.; Haynes, C. J. E.; Light, M. E.; Moore, S. J.; Tong, C. C.; Davis, J. T.; Harrell, W. A., Jr. *Chem. Commun.* **2010**, *46*, 6252.
(21) (a) Caltagirone, C.; Hiscock, J. R.; Hursthouse, M. B.; Light, M. E.; Gale, P. A. *Chem.—Eur. J.* **2008**, *14*, 10236. (b) Jia, C.; Wu, B.; Li, S.; Yang, Z.; Zhao, Q.; Liang, J.; Li, Q. S.; Yang, X. J. *Chem. Commun.* **2010**, *46*, 5376. (c) Jia, C.; Wu, B.; Li, S.; Huang, X.; Zhao, Q.; Li, Q. S.; Yang, X. J. *Angew. Chem., Int. Ed.* **2011**, *50*, 486. (d) Dey, S. K.; Das, G. *Dalton. Trans.* **2011**, *40*, 12048.
(22) Stephenson, A.; Argent, S. P.; Riis-Johannessen, T.; Tidmarsh, I. S.; Ward, M. D. *J. Am. Chem. Soc.* **2011**, *133*, 858.
(23) Scherer, M.; Caulder, D. L.; Johnson, D. W.; Raymond, K. N. *Angew. Chem., Int. Ed.* **1999**, *38*, 1588.
(24) Reaction of L1 with $ZnSO_4$ in $MeOH/H_2O$ led at room temperature to the immediate formation of an insoluble precipitate, which was converted very slowly (over a few months) into the crystalline $[Zn_4(L1)_6(SO_4)](SO_4)_3$ cage, as confirmed by a partially refined single crystal X-ray structure.
(25) Sulfite appears to get oxidized to sulfate over time, which then templates the cage.
(26) A similar observation of metal phosphate formation leading to decomposition of a self-assembled tetrahedral cage was made recently: El Aroussi, B.; Guenee, L.; Pal, P.; Hamacek, J. *Inorg. Chem.* **2011**, *50*, 8588.
(27) Within the dinegative oxoanion series, the intensity of the ESI-MS peaks corresponding to the cage decreased in the order $SO_4^{2-} > SeO_4^{2-} > CrO_4^{2-} > MoO_4^{2-}$.
(28) A viscosity η value of $(1.54 \pm 0.09) \times 10^{-3}$ Pa/s was estimated for the 2:1 v/v CD_3OD-D_2O solvent mixture at 298 K: Wolf, D; Kudish, A. I. *J. Phys. Chem.* **1980**, *84*, 921.
(29) Such a comparison needs to be done with caution, as the Stokes−Einstein equation applies strictly to spherical molecular species. For **2a**, r was estimated here as the radius of the sphere defined by the random tumbling of the tetrahedral cage in solution. As such, r is the distance between the center of the tetrahedron and the farthest H atom belonging to the *t*Bu groups.
(30) Cohen, Y.; Avram, L.; Frish, L. *Angew. Chem., Int. Ed.* **2005**, *44*, 520.
(31) Hallwass, F.; Silva, R. O.; Goncalves, S. M. C.; Menezes, P. H.; Simas, A. M. *Ann. Magn. Reson.* **2004**, *3*, 45.
(32) The buffering was necessary to ensure the EO_4^{2-} anions, particularly the more basic chromate, molybdate, and tungstate, were completely deprotonated.
(33) Smith, R. M.; Martell, A. E., *Critical Stability Constants*; Plenum: New York, 1975.
(34) Marcus, Y. *J. Chem. Soc., Faraday Trans.* **1991**, *87*, 2995.
(35) The average hydrogen-bond acceptor angle for tetrahedral oxoanions was found to be about $122 \pm 12°$ from a Cambridge Structural Database survey. Hay, B. P.; Dixon, D. A.; Bryan, J. C.; Moyer, B. A. *J. Am. Chem. Soc.* **2002**, *124*, 182.
(36) Moyer, B. A.; Delmau, L. H.; Fowler, C. J.; Ruas, A.; Bostick, D. A.; Sessler, J. L.; Katayev, E.; Pantos, G. D.; Llinares, J. M.; Hossain, M. A.; Kang, S. O.; Bowman-James, K. Supramolecular Chemistry of Environmentally Relevant Anions. In *Advanced Inorganic Chemistry*; van Eldik, R., Bowman-James, K., Eds.; Elsevier: Oxford, 2006; Vol. *59*, p 175.